LOW-EARTH ORBIT EFFECTS ON ORGANIC COMPOSITE MATERIALS FLOWN ON LDEF*

Pete E. George
Boeing Defense & Space Group
Seattle, WA 98124–2499 M/S 73–09
Phone: 206/234–2679, Fax: 206/237–0052

Harry W. Dursch
Boeing Defense & Space Group
Seattle, WA 98124–2499 M/S 82–32
Phone: 206/773–0527, Fax: 206/773–4946

SUMMARY

Over 35 different types of organic matrix composites were flown as part of 11 different experiments onboard the NASA Long Duration Exposure Facility (LDEF) satellite. This materials and systems experiment satellite flew in low-Earth orbit (LEO) for 69 months. For that period, the experiments were subjected to the LEO environment including atomic oxygen (AO), ultraviolet (UV) radiation, thermal cycling, microvacuum, meteoroid and space debris (M&D), and particle radiation. Since retrieval of the satellite in January of 1990, the principal experiment investigators have been deintegrating, examining, and testing the materials specimens flown.

The most detrimental environmental effect on all organic matrix composites was material loss due to AO erosion. AO erosion of uncoated organic matrix composites (OMC) facing the satellite ram direction was responsible for significant mechanical property degradations. Also, thermal cycling-induced microcracking was observed in some nonunidirectional reinforced OMC's. Thermal cycling and outgassing caused significant but predictable dimensional changes as measured in situ on one experiment.

Some metal and metal oxide-based coatings were found to be very effective at preventing AO erosion of OMC's. However, M&D impacts and coating fractures which compromised these coatings allowed AO erosion of the underlying OMC substrates.

This paper summarizes the findings for organic matrix composites flown on the LDEF and identifies the LEO environmental factors, their effects, and the influence on space hardware design factors for LEO applications.

BACKGROUND

The benefits of OMC's in spacecraft applications include: (1) significant weight savings, which result in lower launch costs or increased payload; (2) the ability to tailor the coefficient of

* Testing of Boeing composites flown on LDEF was funded by Boeing IR&D. All other Boeing activities were supported by NASA Langley Research Center contracts NAS1-18224 and NAS1-19247.

thermal expansion, thereby providing a structure with dimensional stability; and (3) high stiffness. Because composite laminate properties can be varied by altering the fiber, resin, and laminate layup, a wide range of mechanical and thermal properties can be achieved. Some of the more promising space applications for OMC's include truss structures, frames, booms, solar arrays, and monocoque shell structures.

OMC's have been used in many space applications, but only with extreme caution and a conservative design approach as required with relatively new materials in a space environment. Therefore, the full advantages of OMC's in spacecraft applications have not yet been realized. Because of these advantages, many OMC's were included in both active and passive experiments on LDEF.

LDEF was deployed on April 7, 1984, in LEO at an altitude of 482 km and retrieved January 12, 1990, at an altitude of 340 km. During the 5.8-year mission, the LDEF experienced the following LEO environments:

Atomic Oxygen—ram facing fluence of 9E+21 atoms/cm^2. The higher AO concentrations at lower altitudes resulted in roughly 50 percent of the AO fluence occurring in the last 6 months of the mission.

Solar UV—Cumulative equivalent Sun hours ranged from 4,500 h at LDEF's Earth end to 11,000 h at leading and trailing edges to 14,500 h at the space end.

Thermal Cycling—32,422 ninety-minute cycles. Actual on-orbit measured LDEF structure temperatures ranged from +35 °F to +134 °F. Composite specimen temperatures were a function of both location on LDEF and optical properties. For example, bare composites on the leading edge had a predicted temperature range of –70 °F to +235 °F, while nearby coated composite specimens had a predicted range of –75 °F to +60 °F.

Meteoroid and Space Debris—LDEF had ≈35,000 impact craters with over 3,100 craters >0.5 mm in diameter. The largest crater on LDEF had a diameter of 5.25 mm.

Particle Radiation—The total exposure of LDEF was below the threshold for observable radiation effects in composites. The predicted surface electron dose was ≈300,000 rads.

Figure 1 is a photo of one of The Aerospace Corporation's trays that contained numerous composite specimens provided by several principal investigators. Table 1 lists all the OMC specimens flown, along with their position on the satellite, environment, experiment number, and principal investigator.

POSTRETRIEVAL EXPERIMENT INVESTIGATION

Since the retrieval of LDEF, experiment investigators have been extracting useful design data and observations from the material specimens. Figure 2 shows the general flow for the phases of postretrieval materials experiment investigations. Currently, most OMC specimen testing has been completed, and the results are being reported in relation to the environmental exposures received.

Deintegration and initial observations revealed the significant effects of AO erosion on leading-edge-located OMC's. Trailing edge specimens appeared relatively unchanged with the exception of occasional discolorations due to nearby contamination sources. As a whole, OMC's appeared to have survived relatively intact.

More detailed observations and nondestructive testing revealed that non-AO-exposed graphite-reinforced-OMC specimens were in excellent condition. Non-AO-exposed, glass-reinforced organic matrix composite specimens displayed heavy discoloration due to UV exposure. AO-exposed, graphite-reinforced specimens displayed significant loss of material due to AO erosion up to 0.005 inch for ram facing specimens. AO-exposed, glass-reinforced specimens displayed erosion only through the surface resin layer. The glass fibers then shielded the underlying material, whereas the graphite fibers, due to their AO erosion, provided minimal shielding.

Analysis of dimensional stability data collected on-orbit revealed dimensional changes as a result of both outgassing and thermal cycling (ref. 1). Results for on-orbit measurements of 90° direction strain versus temperature of unidirectional fiber-reinforced organic composited revealed a 40-day period of changing coefficient of thermal expansion (CTE) as the specimen outgassed. The CTE asymptotically approached and reached the preflight value during these 40 days. Moisture desorption was cited as the most likely cause of the shrinkage and changing CTE. On-orbit measurement of 0° CTE did not reveal any significant changes. These results verified the investigators' ground-based simulation predictions. These dimensional changes must be factored into the design of low distortion OMC laminates.

Destructive mechanical testing of non-AO-exposed graphite reinforced materials revealed no significant property changes. AO-exposed specimens displayed reductions in mechanical properties commensurate with the loss of material due to AO erosion. No bulk chemical changes were found for the matrix resins, implying that the environmental effects were only skin deep for the remaining material.

Various coatings were found to be effective at preventing AO erosion of the OMC substrates. Thermal control coatings may have also prevented microcracking by reducing temperature extremes and thermal shocks during thermal cycling. All coatings were subjected to compromise by micrometeoroid and debris impacts which, in addition to allowing AO attack of the OMC substrate, also created delaminations and interply cracking.

ENVIRONMENTAL EFFECT—DESIGN FACTOR RELATIONSHIPS

The hardware designer for spacecraft applications must think in terms of key parameters to design an efficient and reliable structure. Factors such as stiffness and strength can be subject to change due to environmental effects in LEO. Figure 3 is a nonprioritized list of the more significant space hardware design parameters, potential environmental effects, and the LEO environments responsible for those effects. A great deal has been learned about the relationships between these factors and the magnitude of the relationships.

LEO environments for OMC's depend a great deal on hardware location onboard the spacecraft. These environments can be divided into five categories: (1) manned spacecraft interiors; (2) AO- and UV-shielded spacecraft exteriors; (3) AO-shielded, UV-exposed spacecraft exteriors (trailing edge environment); (4) UV-shielded, AO-exposed spacecraft exteriors (backside of solar array panels, Sun tracking satellites); and (5) AO- and UV-exposed spacecraft exteriors (ram

facing environments). The first category is not addressed here as no LDEF specimens were flown in such an environment. Also, this is a relatively benign environment as required for human life support. The last three categories also include effects from the micrometeoroid and debris environment. No specimens were flown with AO exposure and UV shielding. Therefore, category 4 is not addressed except for possible future work to look for synergistic AO and UV effects.

Both the thermal and microvacuum environments exist to some extent in each of the four exterior categories. The synergistic effects of these two environments result in significant, but predictable, dimensional stability concerns for LEO-exposed OMC's. Dimensional changes can occur as a result of outgassing and thermal expansion. Figure 4 shows the dimensional changes as measured on orbit as a function of temperature as part of experiment A0180 by Tennyson et al (ref. 1). Dr. Tennyson and company have shown that these changes are predictable (ref. 2). These two environments also result in outgassing which can be a concern for contamination reasons. OMC specimens on a number of experiments were subjected to outgassing tests which revealed similar values for pre- and postflight testing of epoxies, polysulfones, and polyimides. This suggests that outgassing occurring in space is due to absorbed moisture and not solvents or low-molecular-weight prepolymer species.

AO- and UV-Shielded Environments

Figure 5 lists the predominant environments, effects, and influenced design parameters along with their relationships for AO- and UV-shielded locations. The LDEF specimens shielded from AO and UV were either mounted on the interior of LDEF or as witness specimens on the backside of trays holding exposed specimens. The two predominant environments for these shielded specimens is thermal cycling and microvacuum. Due to LDEF's nonpolar LEO orbit, the particle radiation environment seen by both shielded and exposed specimens was below the observable threshold for composites. While not as extreme as if exposed directly to the LEO environment, the thermal cycling seen by shielded OMC's combined with the microvacuum conditions can result in the following design conditions: (1) microcracking resulting in changes in thermal and mechanical properties and (2) outgasssing resulting in significant, but predictable, dimensional changes. Results from testing of LDEF specimens exposed to this environment showed no mechanical property changes.

AO-Shielded, UV-Exposed Environments

The LDEF satellite flew in a gravity-gradient stabilized orientation, maintaining the same position relative to the direction of motion. As the atmosphere at mission altitudes consists primarily of AO with a mean free path on the order of meters, the satellite swept a clean path through the AO. Therefore, the backside of the satellite received virtually no AO exposure. OMC specimens located on the backside of LDEF were in an AO-shielded, UV-exposed environment.

Figure 6 lists the predominant environments, effects, and influenced design parameters along with their relationships for AO-shielded and UV-exposed locations. These factors and relationships include those discussed previously (identified as grey in Figure 6) and new ones (black) associated with UV exposure and micrometeoroid and space debris. Dimensional stability and outgassing concerns still exist for OMC materials used in this type of environment.

The effects of meteoroid and debris impacts can be devastating for any material depending on the size and velocity of the impactor. However, for OMC specimens flown on LDEF, no specific mechanical property reductions were attributable to impacts. Although fiber breakage and minor delaminations were reported by a number of investigators (refs. 2,3), Whittaker et al. reported no tensile test breakage initiated or culminated on any impact site. It appears that no direct mechanical property influence data from impacts will be available from LDEF OMC specimens. However, documentation of impact damage patterns will allow ground-based testing to simulate these and larger impacts.

No mechanical property changes were attributed to UV exposure effects. Figure 7 shows the flexural strength and modulus results for both control and flight specimens (ref. 4). No significant changes were found for these materials as well as other graphite-reinforced OMC's. Glass-reinforced OMC's flown in AO-shielded, UV-exposed positions did display visible signs of UV degradation.

Optical property changes were observed for AO-shielded, UV-exposed OMC specimens. Table 2 shows pre- and postflight values for absorption and emittance properties for three different OMC materials (ref. 4). Sets of these materials were flown at both the leading and trailing edge of the satellite. The trailing edge specimens which received UV radiation only (no AO) displayed significant increases in emittance (ε). Figure 8 is a thin section photomicrograph of one of the trailing edge specimens. This section, which is illuminated by transmitted light, clearly shows some surface discoloration in the matrix resin with the fibers shielding underlying material. These findings explain the change in optical properties with no measured change in mechanical properties.

Based on LDEF results, exposure to the LEO UV environment without AO exposure does not significantly alter the functionality of graphite-reinforced OMC's. The only possible UV effects are on optical properties. However, provisions must be made for the other environments present in these locations, such as meteoroid and debris, thermal cycling, etc.

AO- and UV-Exposed Environments

The most severe combination of environmental effects for LDEF specimens existed on the leading edge or front side of the satellite. This area received all the environments discussed so far plus highly reactive AO. Figure 9 shows the predominant environments, effects, and influenced design parameters along with their relationships for AO- and UV-exposed locations. Previously discussed factors and relationships are shown in grey, with the additional factors and relationships shown in black. AO erosion was found to be the most severe of all environmental effects for OMC's.

Table 2 lists the optical properties for leading edge exposed graphite-reinforced OMC's. All specimens showed a significant increase in emittance from preflight values, most likely due to surface texturing caused by the AO erosion. Some specimens displayed a thin layer of "ash" while others did not. The C6000 graphite/ PMR-15 polyimide specimens listed in Table 2 did not have this "ash" and displayed significant increases in absorption. Further discussion on the origin of this ash is available elsewhere (refs. 1,6).

Figure 10 shows a photomicrograph of the typical level of AO erosion for leading edge exposed OMC's. The actual erosion level for various OMC specimens distributed around the front side of the satellite varied with angle of exposure to the direction of motion. Reactivity has been calculated at 0.9 to 1.2×10^{-24} cm^3/atom based on recession measurements for graphite/epoxy

specimens by a number of investigators. This resulted in a loss of up to 0.005 inches of material, the equivalent of approximately one ply of laminate.

For unidirectionally reinforced specimens, the reduction in mechanical properties was found to be proportional to the reduction in specimen cross-sectional area. Therefore, as shown in Figure 11 for the AO and UV exposed T300 graphite /934 epoxy specimens flown on M0003-8, there was little change in modulus based on postflight specimen cross-sectional area. Strength values may have been effected by AO erosion-created stress concentration sites. Although useful for determination of lamina properties, unidirectional layups are rarely used in real applications due to the highly isotropic nature of the material.

A better indication of OMC mechanical property performance in AO environments is given by the test values from nonunidirectionally reinforced specimens. The results shown for C6000 graphite/PMR 15 epoxy in Figure 11 reveal a significant drop in both strength and modulus. These reductions are based on a postflight specimen cross section indicating losses due to more than thickness reduction. The loss of a surface 0° oriented ply greatly reduces stiffness and strength properties as only a portion of the plies are in the 0° direction for typical layup. Also, for optimization of bending stiffness, 0° plies are often placed at or near the surface of a laminate. For AO-eroded specimens, this will result in greater reduction in bending stiffness and an imbalanced layup with bending-stiffness coupling during loading. These specimens also displayed minor warpage due to the erosion of the surface 0° direction ply.

In most exterior spacecraft applications which require the high stiffness and dimensional stability of graphite-reinforced OMC's, the type of environmental effect experienced by AO-exposed LDEF OMC's is clearly unacceptable. In addition, expected AO fluences for future long-term LEO missions such as Space Station *Freedom* are many times that experienced by LDEF. OMC's used in these applications will require protective coatings.

AO- and UV-Exposed OMC's with Protective Coatings

Figure 12 shows the predominant environments, effects, and influenced design parameters along with their relationships for effectively coated OMC's in AO- and UV-exposed locations. If fully effective against AO and UV attack, the influence of environmental factors on design concerns is reduced to those discussed in the previous section on AO and UV shielded OMC's.

The full impact of the LEO AO environment on organic materials became evident during early shuttle missions and LDEF integration occurred before this realization. Fortunately, a number of OMC specimens were flown on LDEF with various coatings. These coatings were primarily intended for thermal control but many of them offered excellent protection against AO erosion.

Experiment A0134 contained T300 graphite/ 934 epoxy specimens coated with a thin sputtered coating of 600 Å of SiO_2 over 1,000 Å of nickel (ref. 5). This coating was effective in preventing AO caused erosion of the composite substrate. Figure 13 shows the large 11.75- by 16.75-inch T300 graphite/ 934 epoxy specimen flown as part of M0003-8. This panel was divided into four quadrants with one quadrant uncoated and the other three quadrants coated with A-276 white polyurethane, Boeing Materials Standard (BMS) 10-60 white polyurethane, or Z-306 black polyurethane. Although some coating thickness loss was observed for the white polyurethane coatings, the TiO_2 and talc pigments and fillers accumulated on the surface, providing an effective

AO barrier. The Z-306 coating with organic carbon filler underwent AO caused degradation resulting in loss of composite material.

Figure 14 is a three-dimensional plot of the data collected during a laser profilometry raster scan of a portion of the panel shown in Figure 13. The data are plotted as a 0.0005-inch grid for the x-y plane and 0.001-inch line segments of various thicknesses for the z-direction (depth). The approximately 1-in^2 area contains a circular region shielded from AO attack by a mounting washer on the surface. An A276 white polyurethane coating covers the rear left half of the panel segment. The A276 coating was clearly effective at preventing AO erosion of the underlying OMC substrate. However, AO erosion was observed by different investigators in areas where the protective coatings had been breached by impacts or cracks.

Figure 15 shows the effectiveness of coatings possessing optimum optical properties for the minimization of thermally induced microcracking of the composite substrate. This is accomplished by passively controlling the thermal cycling extremes and thermal shock seen by the underlying composite substrate. This figure shows the postflight measured microcrack density versus thermal cycling conditions for the coated composite panel shown in Figure 13 (ref. 3). Crack density is measured from polished cross sections at $\times$ 200 magnification. Thermal cycling conditions were estimated using LDEF environmental data (ref. 6), physical and optical properties, and recorded flight data for an underlying structure. The increased crack density for the more severely cycled material is most likely due to the thermal shock as the energy input was into one side of the specimens in the form of solar exposure. No inflight measurement of dimensional stability versus microcracking data is yet available. However, the impact of microcracking on dimensionally critical spacecraft hardware has been a design issue in past experiences such as the Hubble space telescope optical truss assembly.

The significance of these findings is that microcracking was prevented by reducing the thermal cycling extremes and shock, in this case through the use of reflective optical coatings.

AO- and UV-Exposed OMC's with Breached Protective Coatings

While a number of coatings were found to be effective at preventing AO attack, micrometeoroid and debris impacts along with thermal-stress-induced cracks did expose OMC substrates allowing AO erosion. Figure 16 shows the factors and relationships for AO- and UV-exposed coated OMC's with a coating breach. Compromising the coating brings back the concerns with unprotected OMC materials in this type of environment. The level of concern is tied to the severity of expected coating removal due to impacts and/or cracking.

Figure 17 shows a cross-section photomicrograph of an LDEF A-276 coated graphite/epoxy specimen taken from a large panel with a meteoroid or debris impact. Near the sides of the photomicrograph the coating has effectively prevented AO erosion of the substrate. However, at the impact site, in addition to the impact damage, the jagged pattern of AO erosion is plainly visible on exposed OMC surfaces.

The area of the panel effected by these impacts was less than 0.01 percent, and the total volume of the OMC material effected by the impacts and erosion was less than 0.000001 percent. This suggests that OMC's can be adequately protected with coatings for many LEO applications. Straightforward design calculations, based on anticipated meteoroid and debris environments and

AO fluences combined with AO reactivity data, can be performed by the space hardware designer to determine if coated OMC's can be used.

CONCLUSIONS

The data and observations generated from LDEF organic matrix composite experiments will greatly increase the spacecraft hardware designers confidence for using these materials in LEO applications. OMC's used in high atomic-oxygen exposure environments will require protective coatings. However, LDEF results show that adequate coatings are available. OMC's used in low or zero AO-exposure environments may not require coatings or shielding based on AO erosion rates, meteoroid and debris protection, and thermal control requirements.

The main design considerations for AO exposed coated OMC's relative to the LEO environment include (1) outgassing/ microcracking-induced dimensional changes, (2) coating optical properties and AO/UV resistance, (3) impact damage and subsequent AO erosion effects on mechanical properties, and (4) contamination from outgassing. No detectable mechanical or chemical property changes have been reported for AO-shielded composites. Glass-reinforced OMC's may not require protective coatings as the surface layer of glass fibers protects underlying material. However, UV degradation is more significant with glass reinforced OMC's.

The main design considerations relative to low or zero AO-exposed uncoated OMC's relative to the LEO environment include (1) AO erosion rate (0.9 to 1.2×10^{-24} cm^3/atom for graphite/ epoxy at 60-percent fiber volume, similar for other graphite OMC's); (2) impact damage; (3) outgassing/ microcracking-induced dimensional changes; (4) AO- and UV-induced optical property changes, and (5) contamination from outgassing. Graphite-reinforced OMC's were found to have some inherent UV resistance. No bulk chemical changes have been reported for both AO- and UV-exposed, graphite-reinforced OMC's.

FUTURE WORK

The largest potential payoff for LDEF data relative to all materials may not be in directly applied design information but in verification of simulation and modeling techniques. This will allow ground-based evaluation of new materials developed since the integration of LDEF.

Future OMC materials development efforts based on LDEF results should focus on microcrack resistance, low outgassing, and AO resistance along with dimensional stability modeling. Also, increased matrix polymer AO resistance would reduce post-impact substrate erosion of coated OMC's in high AO-fluence, long-term missions.

REFERENCES

1. Tennyson, R. et al: "Preliminary Results From the LDEF UTIAS Composite Materials Experiment." First LDEF Post Retrieval Symposium, NASA CP-3134, February 1992.

2. Tennyson, R., and Manuelpillai, G.: "Analysis of LDEF Micrometeoroid/Debris Data and Damage to Composite Materials, LDEF Materials Results For Spacecraft Applications." Printed elsewhere in this publication, October 1992.

3. George, P.E., Dursch, H.W., and Hill, S.G.: "Space Environmental Effects on LDEF Composites: A Leading Edge Coated Graphite Epoxy Panel." Second LDEF Post Retrieval Symposium, NASA CP-3194, June 1992.

4. George, P.E., and Hill, S.G.: "Results from Analysis of Boeing Composite Specimens Flown on LDEF Experiment M0003-8." First LDEF Post Retrieval Symposium, NASA CP-3134, February 1992.

5. Slemp, W. S. et al.: "Effects of LDEF Flight Exposure on Selected Polymer Matrix Composite Materials." First LDEF Post Retrieval Symposium, NASA CP-3134, February 1992.

6. Bourassa, R.J., and Gillis, J.R.: "Solar Exposure of LDEF Experiment Trays." NASA Contractor Report No. 189554, February 1992.

Table 1. Organic matrix composites flown on LDEF.

ROW #	ANGLE OFF RAM	AO FLUX x10^21a/sq.cm.	UV ESHx10^3	EXP. NUMBER	PRINCIPAL INVESTIGATOR	MATERIALS
9	8°	8.32	11.1	A0134	Wayne Slemp - NASA La RC (804) 864-1334	5208/T300,934/T300,P1700/C6000,P1700/C3000 930/GY70
				M0003-9	Brian Petrie - Lockeed (408) 742-8244	CE-339/GY70, F263/T50, 934/T50, X904B/T50 E788/T50, 3501-5A/HMS, E788/C6000 934/HMF176, CE-339/E-Glass,F593/P75,934/P75
				M0003-8	Pete George - Boeing (206) 234-2679	934/T300, P1700/T300, PMR15/C6000
10	22°	7.78	10.7	A0054	TRW	Epoxy/Fiberglass
8	-38°	6.63	9.4	A0171	Ann Whitaker - NASA MSFC (205) 544-2510	934/HMS, 934/P75S, P1700/HMF, Epoxy/ S-Glass
				MOOO3-10 **	Brian Petrie - Lockeed (408) 742-8244	X904B/GY70, 3501-5A/HMS, X904B/E-Glass
				MOOO3-10 **	Thomas Cookson - General Dynamics (619)547-5081	X-30/GY70*,CE-339/GY70, CE-339/P75S 934/P75S, 934/GY70, P1700/W722*, V378A/T300
				M0003-10 **	Charles Smith - McDonnell Douglas (714) 896-4015	5208/T300*, P1700/T300*, PES/T300* Polyimide/C6000*
				M0003-10 **	Pete George - Boeing (206) 234-2679	934/T300, 3501-6/AS, P1700/T300, PMR15/C6000 LARC 160/Graphite
7	-68°	3.16	7.2	A0175	Dick Vyhnal - Rockwell (918) 835-3111 x2252	F178/T300, PMR15/C6000
12	82°	1.2	6.9	A0180	Rod Tennyson - U of Toronto (416) 667-7710	934/T300, 5208/T300, SP288T300 SP328 Kevlar/Epoxy, SP290 Boron/Epoxy
				A0019	David Felbeck - U of Mich. (313) 994-6662	5208/T300 interleafed w/ Kapton
1	112°	0.06	7.5	A0175	Dick Vyhnal - Rockwell (918) 835-3111 x2252	934/T300, LARC 160/C6000
5	-128°	0	8.2	P0005	Dean Lester - Morton Thiokol (801) 863-6809	carbon/carbon, Epoxy/graphite, Epoxy/Kevlar Epoxy/Glass (all mounted internally)
4	-158°	0	10.4	A0054	TRW	Epoxy/Fiberglass
				M0003-10	(See Row 8 List for M0003-10)	
3	172°	0	11.1	MOO03-9	(See Row 9 List for M0003-9)	
				M0003-8	(See Row 9 List for M0003-8)	
				A0138	Heinrich Jabs - Matra Espace France (33)-1-61-39-72-73	934/GY70,V-108/Kevlar, V108/T300, V108/GY70 V108/G837

* Some specimens flown with protective coating

** Part of Advanced Composites experimet Integrated by Aerospace corp. Gary Steckel (213) 336-7116

Table 2. Typical optical property changes for UV-exposed LDEF graphite-reinforced OMC's.

Material	Property	Preflight values	Postflight values Exposed side	
			Trailing	Leading
934 Epoxy/	α =	0.90	0.87	0.93
T300 Graphite	ε =	0.73	0.82	0.93
P1700 Polysulfone/	α =	0.90	0.88	0.93
T300 Graphite	ε =	0.73	0.82	0.93
PMR-15 Polyimide/	α =	0.90	0.90	0.98
C6000 Graphite	ε =	0.73	0.79	0.93

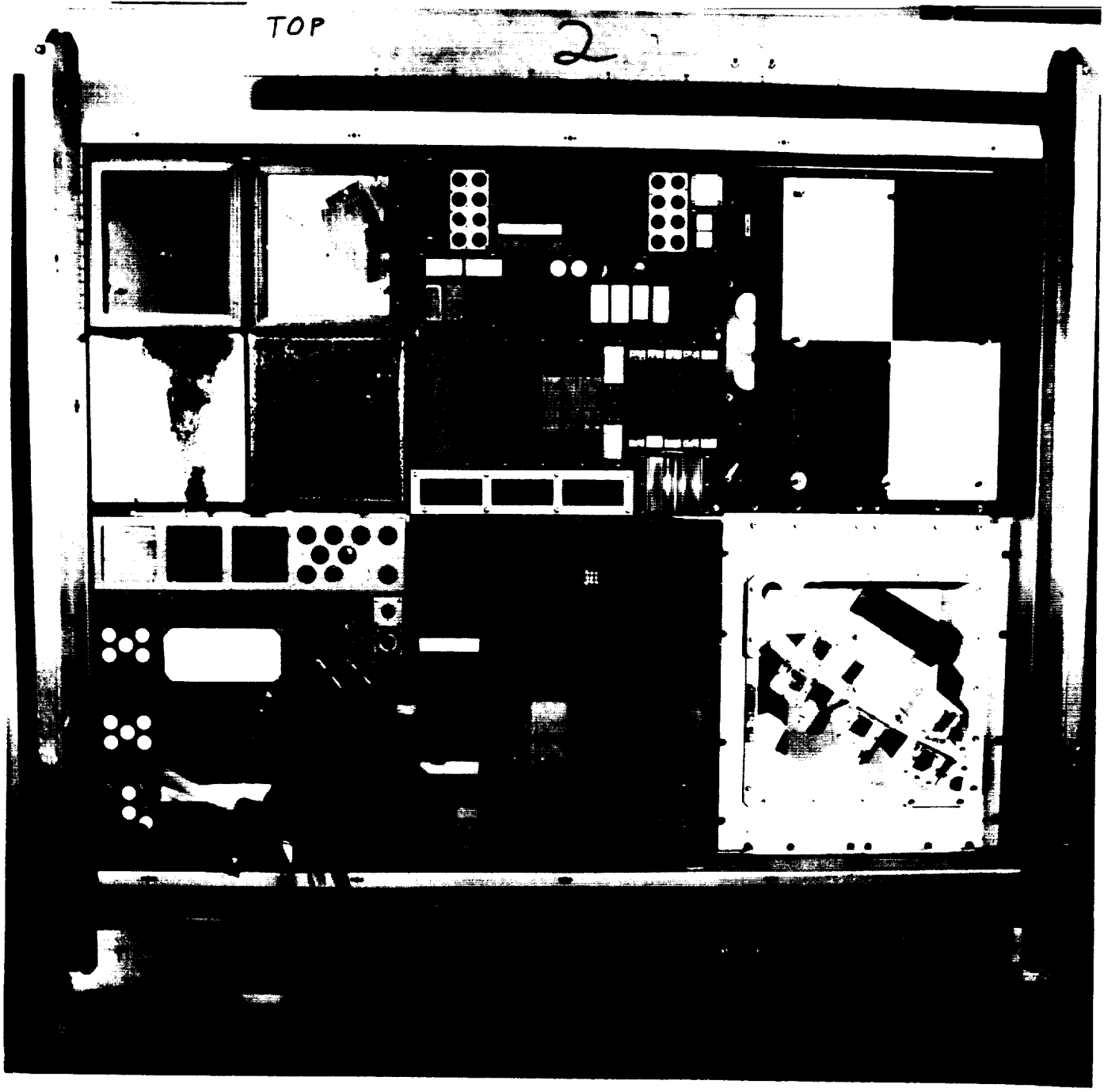

Figure 1. Postflight photograph of experiment M0003 taken by NASA photographers at Kennedy Space Center.

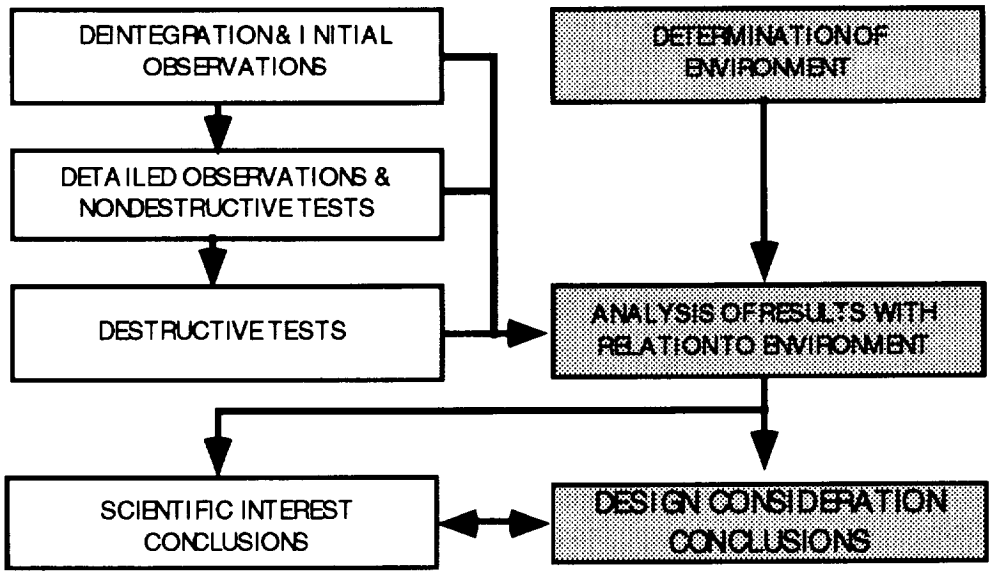

Figure 2. Flow of LDEF materials experiment investigation process.

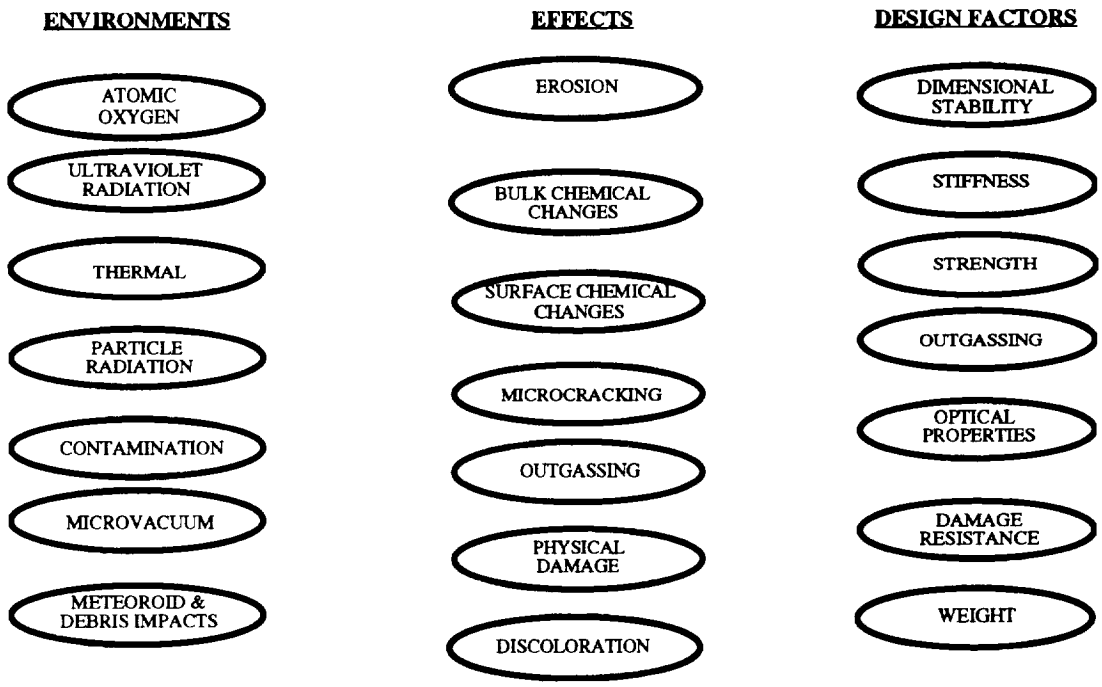

Figure 3. Environments, effects, and design factors for organic matrix composite materials in LEO applications.

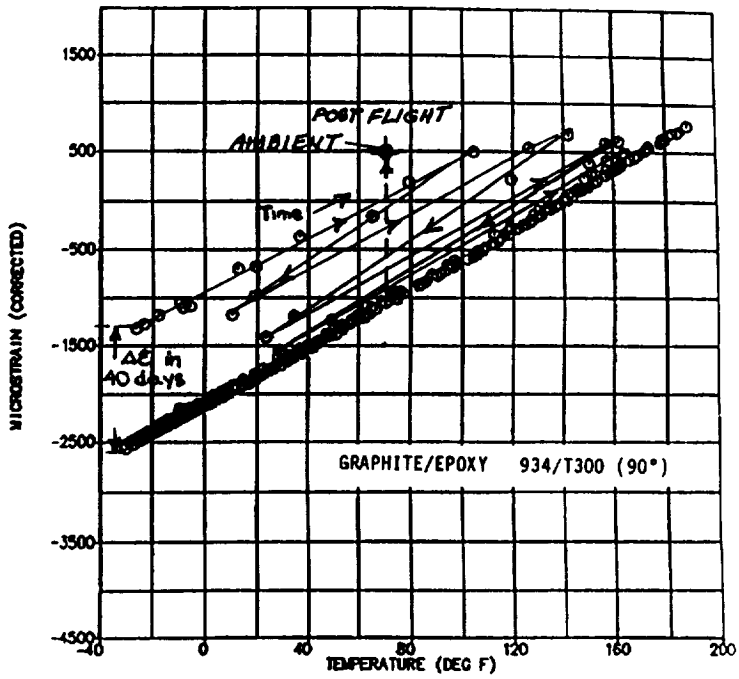

Figure 4. Effects of outgassing and thermal cycling on dimensional stability for an LDEF graphite-reinforced OMC.

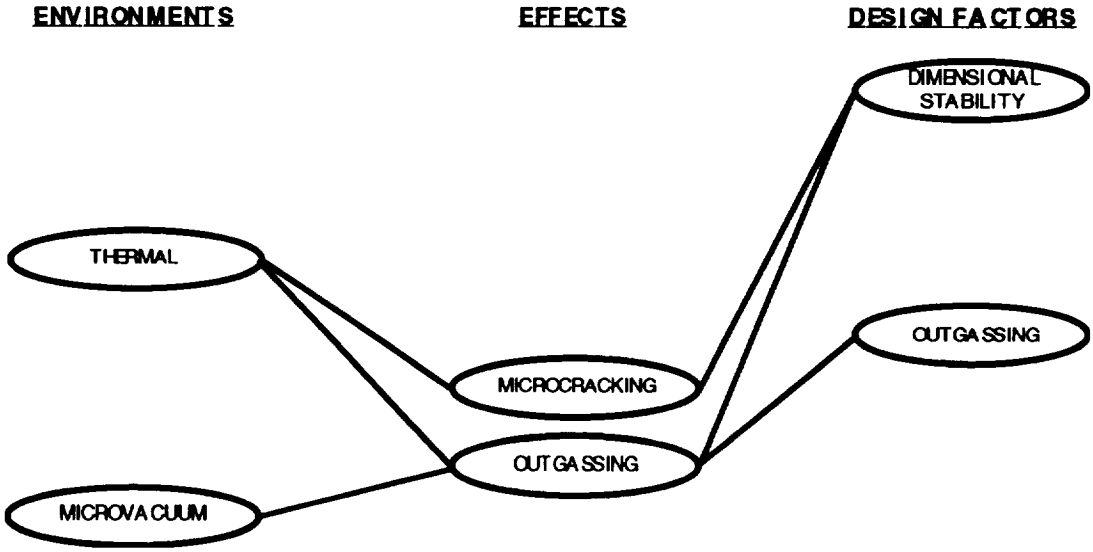

Figure 5. Environmental design factors and relationships for AO- and UV-shielded OMC's in LEO.

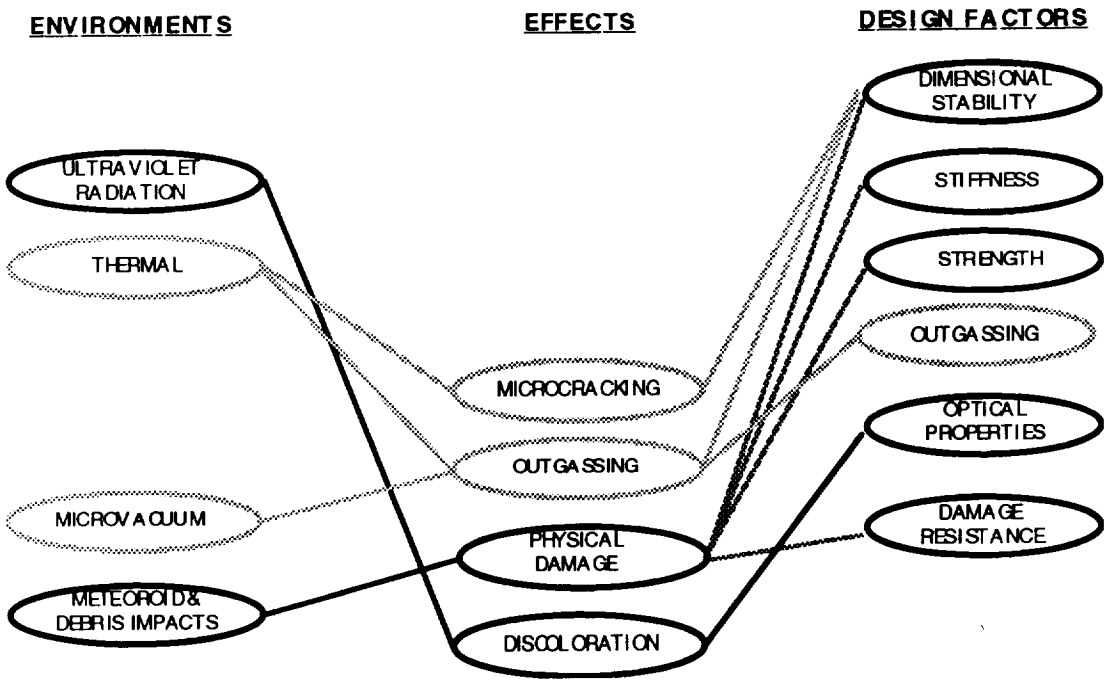

Figure 6. Environmental design factors and relationships for AO-shielded and UV-exposed OMC's in LEO.

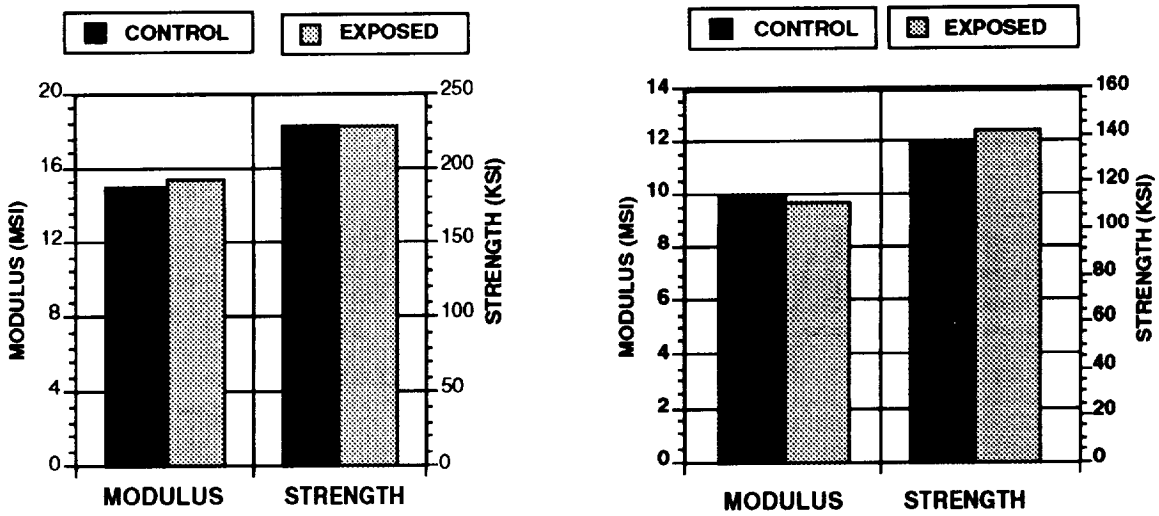

Figure 7. Typical flexural mechanical property changes for AO-shielded, UV-exposed LDEF graphite-reinforced OMC's.

Figure 8. Cross-sectional photomicrograph of UV-exposed LDEF graphite-reinforced OMC showing limited UV degradation.

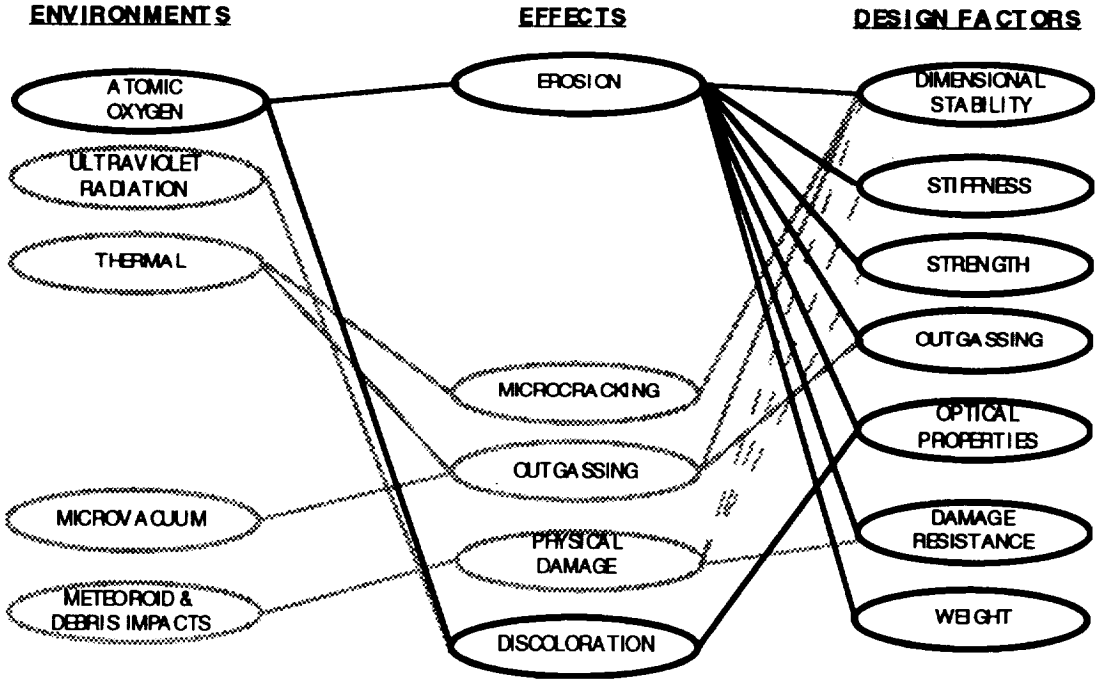

Figure 9. Environmental design factors and relationships for AO- and UV-exposed OMC's in LEO.

Figure 10. Cross-sectional photomicrograph of UV-exposed LDEF graphite-reinforced OMC showing AO erosion.

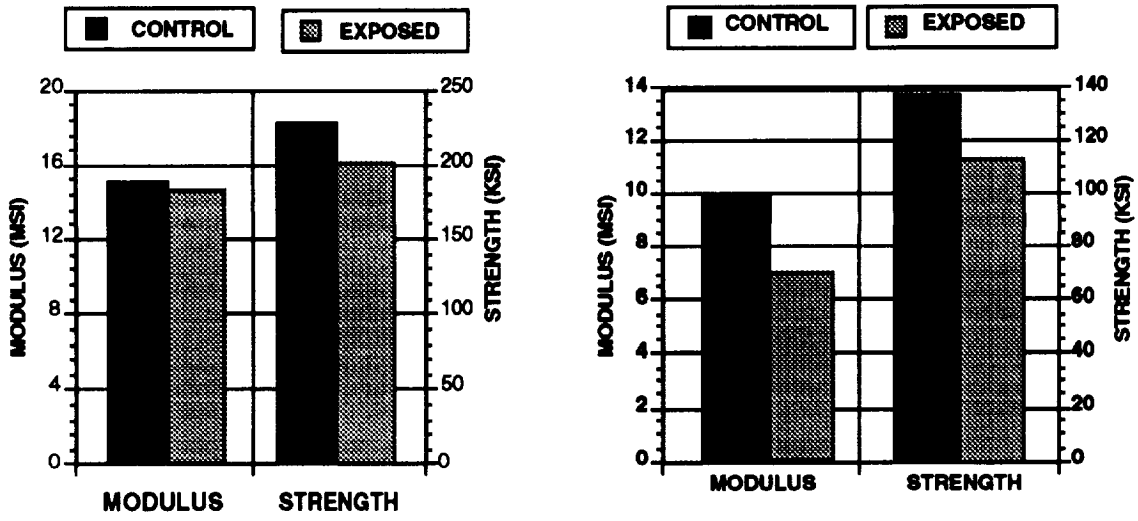

Figure 11. Typical flexural mechanical property changes for AO- and UV-exposed LDEF graphite-reinforced OMC's.

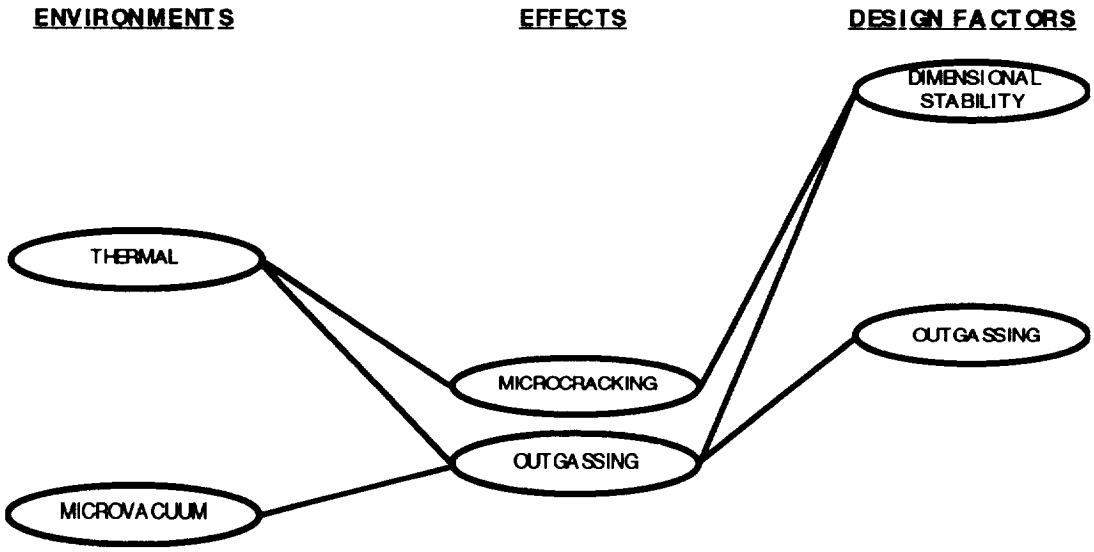

Figure 12. Environmental design factors and relationships for AO- and UV-exposed OMC's with protective coatings in LEO.

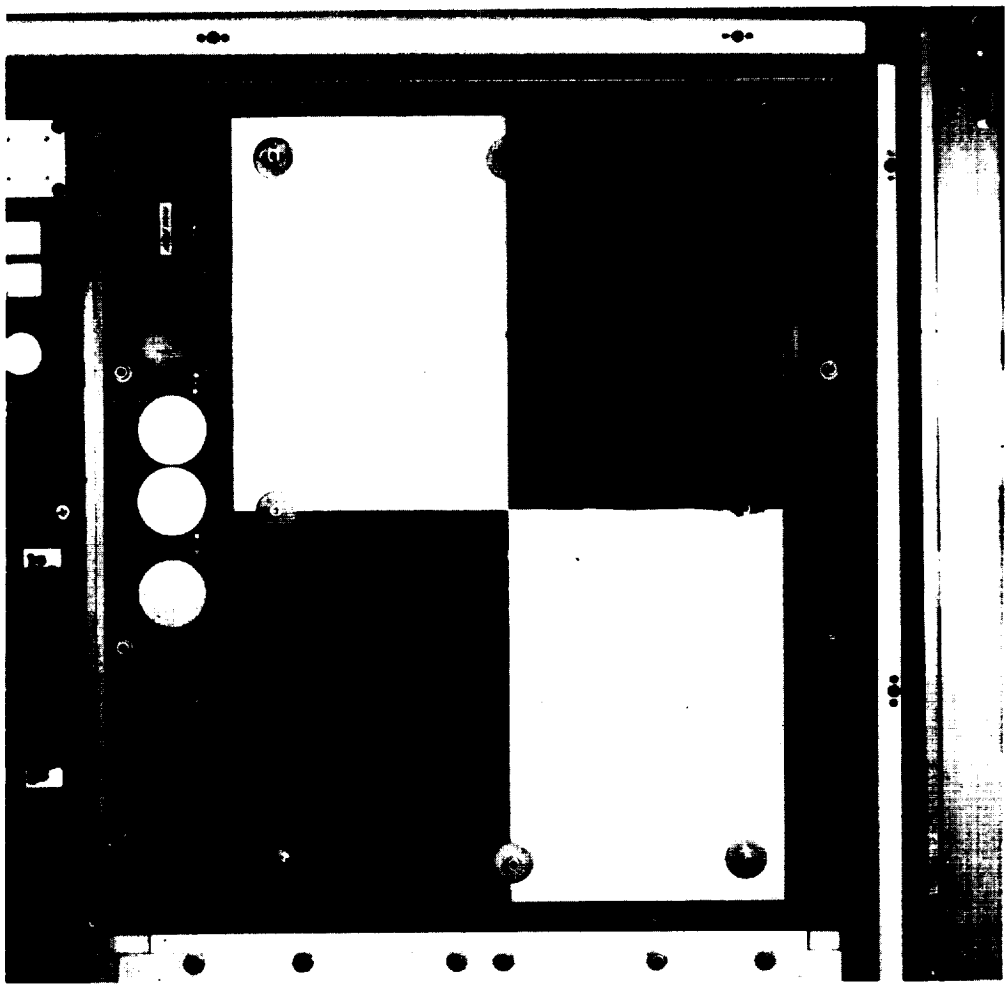

Figure 13. Coated T300 graphite/934 epoxy composite panel.

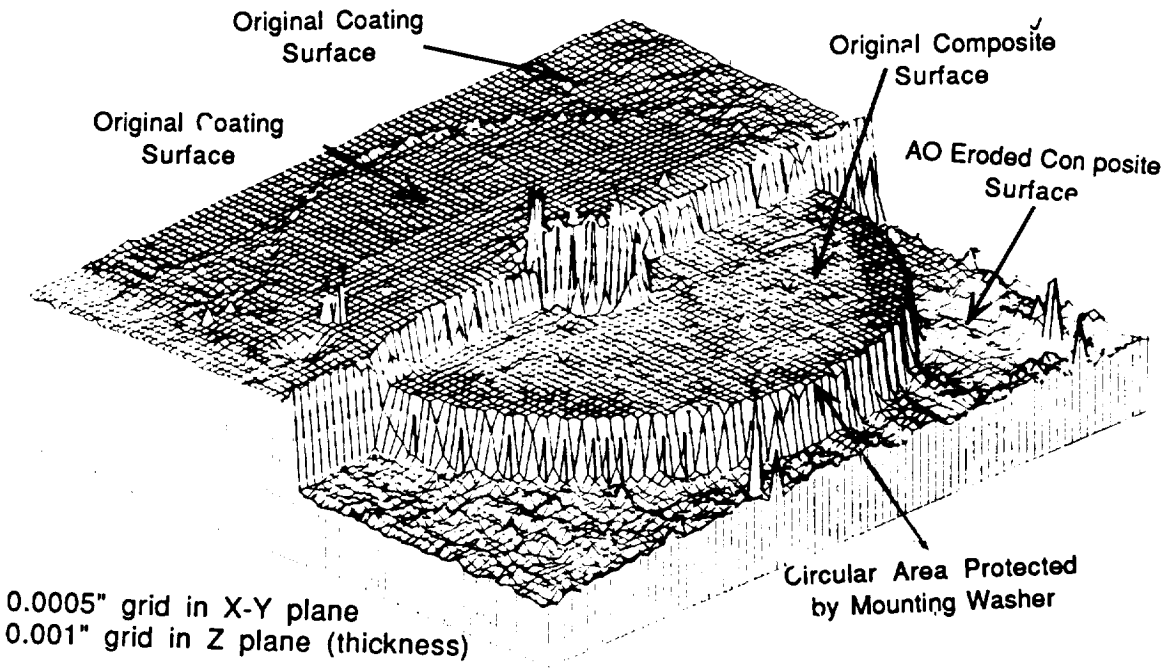

Figure 14. Three-dimensional plot of profilometry measurements taken from a partially coated graphite-reinforced OMC.

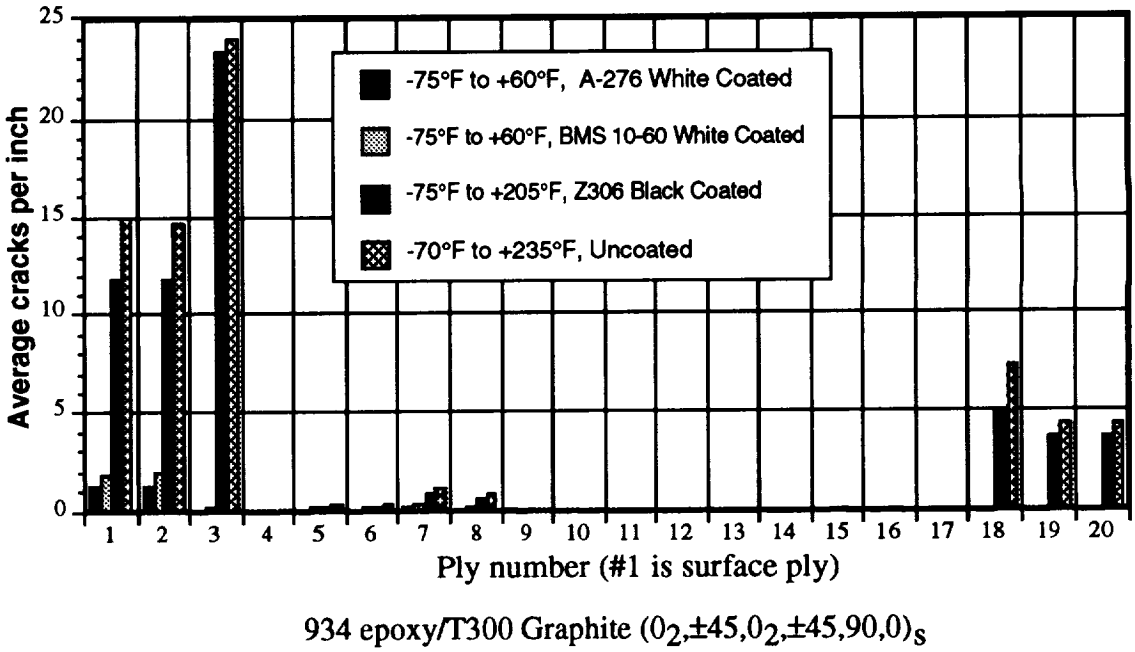

934 epoxy/T300 Graphite $(0_2,\pm45,0_2,\pm45,90,0)_S$

Figure 15. Microcrack density and distribution in an LDEF OMC for various thermal environments.

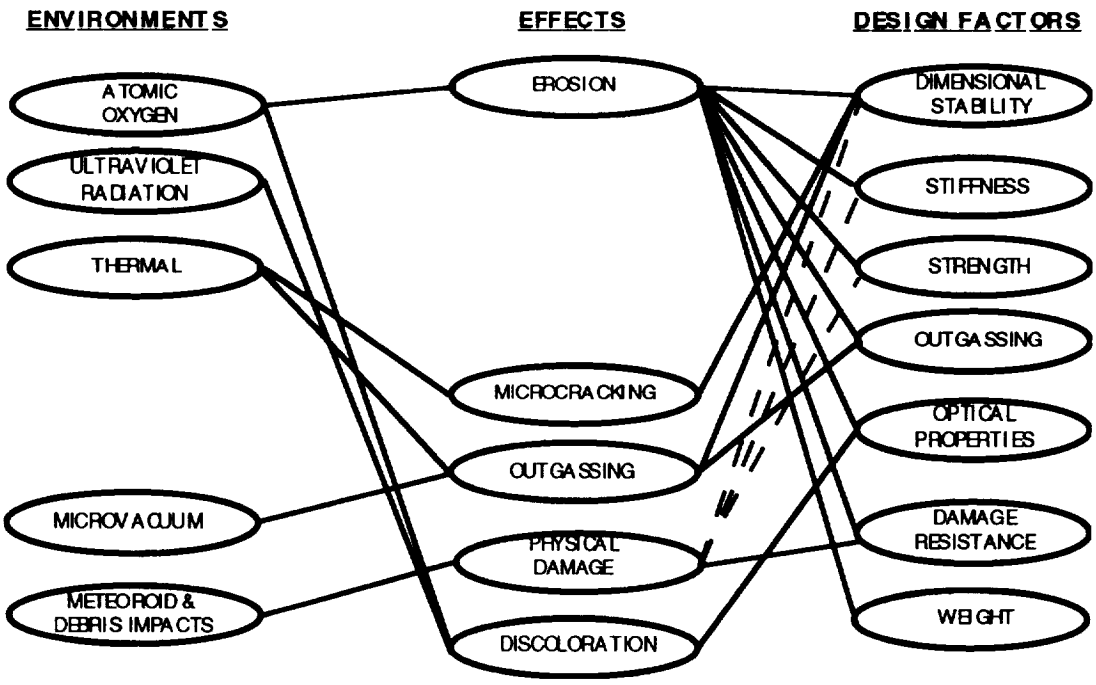

Figure 16. Environmental design factors and relationships for AO- and UV-exposed coated OMC's in LEO with protective coating breach.

Figure 17. Cross-sectional photomicrograph of coated graphite-reinforced OMC showing impact damage and post-impact AO erosion.